CHAPTER 1: Introduction and literature survey

1.1 Introduction

A material absorbs light on irradiation by photons with energy higher than or equal to its bandgap (E_g). The absorbed light photo-excites electrons from the valence band (VB) to the material's conduction band (CB). Electron excitation leaves a positively charged hole (h^+) in the VB and photo-excited electrons (e^-) in the CB. Suppose reactants with appropriate redox potential (relative to the photocatalyst VB) get oxidized by quenching the h^+ in the VB, and species with relevant reduction potential get reduced using the photo-excited CB electrons. In that case, the material is called a photocatalyst. Overall, the oxidized species transfers electrons to the VB, then to the CB, and finally to the reactant reduced.

Since photocatalysis uses renewable light as the energy source for driving reactions, therefore, it is a green technique and is utilized across the world for addressing environmental issues (L.-N. He et al., 2020; Vasilache et al., 2013; Wanjun Wang et al., 2016; J. Yu et al., 2012). Photocatalysts could be (i) homogeneous or (ii) heterogeneous.

Homogeneous photocatalysis requires the photocatalyst and reactants in the same phase during the reaction. The appreciable activity of homogeneous photocatalysts is due to their molecular level dispersion in the reaction medium (Baruah et al., 2018). The primary drawback of homogeneous catalysis is the problem of separating the catalyst from the reaction mixture after the completion of the target reaction. Separation of the catalysts is essential for their reuse. In heterogeneous photocatalysis, solid catalyst

particles in a liquid reaction medium can be separated after use and recycled. Given this, the present thesis concentrates on the development of heterogeneous photocatalysts.

Heterogeneous photocatalysts have been utilized for wastewater detoxification, CO_2 reduction, H_2O_2 production, H_2 production, organic synthesis, etc. (Albero et al., 2020; Gopakumar et al., 2022; Silva et al., 2008; Upadhyay et al., 2014; Xiao et al., 2020). Semiconductor particles with bandgap energies in the UV or the visible range of the solar spectrum have been applied as heterogeneous photocatalysts. But single-phase photocatalysts have several drawbacks.

i) Solar radiation has approximately 42% visible light and less than 5% UV light (X. Chen & Zhu, 2011). Therefore, visible light photocatalysts (with moderate or small bandgaps) can use solar radiation more efficiently than wide bandgap semiconductors to drive chemical reactions.

ii) Lower oxidation and reduction ability: Narrow or moderate bandgap photocatalysts may not be effective for several redox reactions. This problem is due to the photocatalysts' restricted VB and CB positions relative to the concerned reactants.

iii) Recombination problem: The photogenerated h^+ and e^- (oppositely charged) are extremely unstable and reactive. Figure 1.1 displays a schematic representation of a single photocatalyst during a photocatalytic reaction. Either the photoexcited species will recombine or oxidize and reduce suitable reactant molecules. The lifetimes of the photo-excited charges (h^+ and e^-) are small in the single pure photocatalyst. Hence, such materials exhibit diminished photocatalytic activity.

iv) Inappropriate charge separation: Recombination can be prevented by spatial separation of photogenerated charges (e^- and h^+). Such charge separation can enhance the lifetimes of photoexcited species. But there is little possibility of such separation in single-phase photocatalysts.

v) Adsorption properties: The reactants can get reduced or oxidized when they interact favorably with the photocatalyst surface. Hence, appropriate adsorption behavior towards the reactant species makes the photocatalyst more efficient.

Broadly, there are different ways of tackling these issues. One is by forming composites of two photocatalyst components. These materials have a reducing and an oxidizing photocatalytic part. The second way is the cation or anion doping of a single-phase photocatalyst. Another option is to have a doped photocatalyst as a component of a composite photocatalyst.

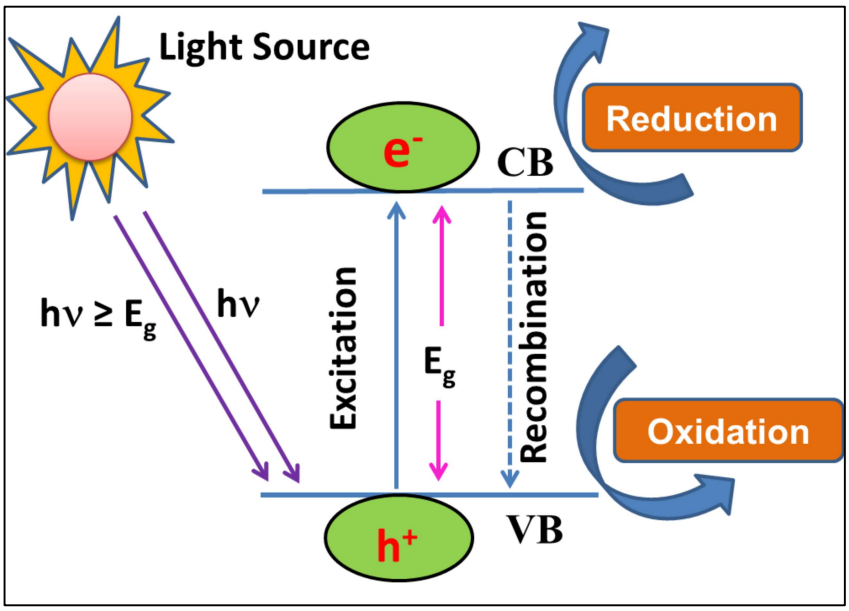

Figure 1.1 Schematic diagram of the single-phase semiconductor photocatalysis.

1.2 Composite photocatalysts

Two or more semiconductors join to form composites or heterostructure photocatalysts. The coupling of two different semiconductors with suitable VB and CB positions can provide better charge separation and distinct adsorption properties. Thus, the synthesis of composite photocatalysts such as AgI/$CuWO_4$, TiO_2/CuS, Fe_3O_4/Cu_2O, NiO/TiO_2, NiS/CdS, etc. have been reported in the literature (Jatav et al., 2021;

Khanchandani et al., 2016; Pal et al., 2022; J. Yu et al., 2010; Jun Zhang et al., 2013). Moreover, the bandgaps of the two components should be staggered to each other because such an arrangement gives better charge separation. There are two types of photocatalyst heterostructures with such staggered band alignments. These are (i) p-n heterojunction and (ii) Z-scheme composite photocatalysts. Figure 1.2 displays the electron transfer modes in these two distinct composite photocatalyst types.

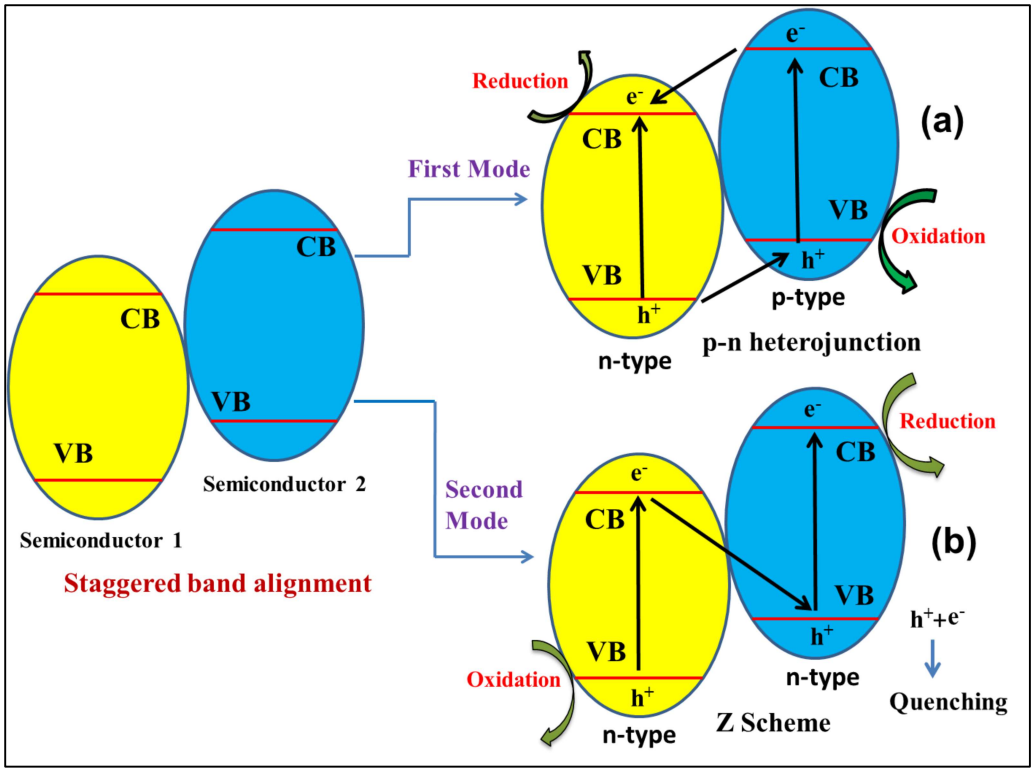

Figure 1.2 The photocatalytic mechanisms followed in (a) p-n heterojunction, (b) Z scheme with staggered band alignment.

1.2.1 p-n heterojunction photocatalyst

A typical p-n heterojunction has p-type and n-type semiconductor components. The excess electrons on the n-type semiconductor side and the holes on the p-type part migrate to the p-n interface. Hence, the electrons tend to diffuse from n-type to p-type until the Fermi level's equilibrium is established (Peng et al., 2014). Thus, an internal

electric field developed at the interface of the heterojunction photocatalyst. Irradiation of such photocatalysts by light with an energy greater than the individual semiconductor bandgaps generates electron-hole pairs. The photoexcited electrons on the more negative CB (the p-type part) move to the relatively positive CB (n-type) component (Figure 1.2a). Likewise, holes move from the more positive VB (n-type) to the less positive one (p-type). Thus, electrons accumulate on the less negative CB and holes on the component with a more positive VB position, separating the charge carriers (Z. Zhang et al., 2010).

1.2.2 Z-scheme photocatalysis

Although the p-n heterojunction exhibits efficient charge separation, the reaction driving forces are small because of the lower oxidation and reduction potentials of the hole-rich VB and the electron-rich CB. A Z scheme photocatalyst can solve this problem. A typical Z scheme photocatalyst is an amalgam of two or more n-type or two or more p-type semiconductors (either n-type or p-type) with staggered band alignments. Irradiation of the photocatalyst with light energy greater than or equal to the bandgap of the component semiconductors induces the generation of photo-excited electrons and holes in both parts of the composite. As depicted in Figure 1.2b, the photo-excited electrons on the CB of one semiconductor quench the VB holes of the second component. At the end, holes accumulate on the more positive VB of one semiconductor and electrons on the more negative CB of the other component. The higher oxidation and reduction potential of the hole-rich VB and the electron-rich CB increases the redox ability of the photocatalyst. Thus, a Z scheme mechanism improves charge separation and the redox ability of the photocatalyst.

1.3 Importance of doping and defects in heterogeneous photocatalysis

As mentioned earlier, doping with a metal or a non-metal ion is another strategy for improving or altering the photocatalytic properties of a single-phase semiconductor. Semiconductor doping intentionally includes foreign elements in the host lattice structure. Doping could be cationic or anionic depending on whether the metal or a non-metal is the included foreign element. The foreign element either substitutes an atom or occupies an interstitial position (void space) in the host lattice structure. Doping can change the electronic structure and adsorption properties. Figure 1.3 displays a schematic of the effect of doping in photocatalysis. Doping induces various defects in the pure material that may improve catalytic activation of a particular bond in a reactant molecule selected for catalysis. Alternatively, the different defects can specifically trap holes or electrons. The latter prevents the quick recombination of photogenerated electrons and holes.

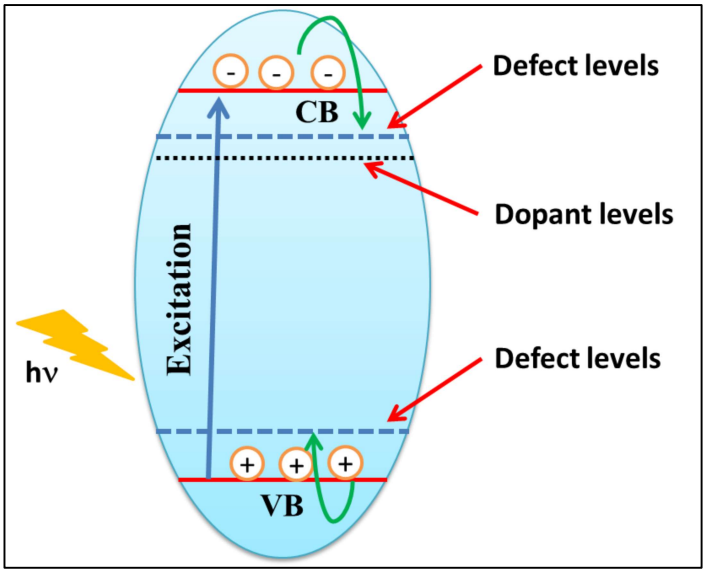

Figure 1.3 Schematic presentation of the effect of doping on photocatalysis.

Oxygen vacancies (OVs) are another frequently encountered defect in metal oxides (Corby et al., 2020; Gunkel et al., 2020; Puigdollers et al., 2017). Generally, OVs originate in two ways. One way is that the lattice oxygen of the oxide can directly go to the gas phase in the form of O_2 (shown in equation 1.1).

$$MO_2 \rightarrow MO_{2-x}(OV\ lattice) + \frac{1}{2}xO_2(gas) \quad (1.1)$$

Another route for OV generation is the chemical reduction of the lattice oxygen to OV. Cation substitution by a lower valent metal dopant could also induce OVs. The generation of OVs can also affect the electronic band structure. For example, the OVs in CeO_2 alter its bandgap and improve the photocatalytic CO_2 reduction efficiency (Hezam et al., 2020). Many research studies demonstrate that OVs can also widen or narrow down the bandgap of the native semiconductor (Ansari et al., 2013; Linderälv et al., 2018; Nachiar & Muthukumaran, 2019). The synergistic effect of doping and OVs can play an important role in determining photocatalyst efficiency. For instance, Zhang et al. found nitrogen doping and OVs together in $Bi_2O_2CO_3$ nanosheets endowed it with enhanced photocatalytic activity towards organic pollutant degradation (Y. Zhang et al., 2016). The photogenerated charge carrier efficiency of TiO_2 was increased by phosphorus doping and OVs (X. Feng et al., 2018). Recently, Pan et al. showed that the bandgap of hematite decreased and improved charge carrier concentration due to doping and OVs (Pan et al., 2020).

The photocatalytic activity also depends on the valence band (VB), and conduction band (CB) edges. The CB and VB edges should be above and below the reduction and the oxidation couple, respectively. Therefore, a suitable bandgap with a proper band edge position is necessary to design an efficient photocatalyst. Doping also can change the electronic structure of the solid photocatalyst (J. He et al., 2010; Koshi et

al., 2022; N. Zhang et al., 2018). It can widen or narrow down the bandgap of the parent photocatalyst (Jain et al., 2006; Joshi et al., 2016; Kalathil et al., 2013). For example, Wang et al. mentioned a detailed DFT investigation of the oxygen doping effect on Ta_3N_5 photocatalyst. The oxygen dopant changed the bandgap and band edges of the parent photocatalyst (Jiajia Wang et al., 2014). Thus, doping can tune the bandgap and the band edges of a photocatalyst, in addition to improved charge separation.

Doped semiconductors can also form a composite with another (semiconductor or metal) component, resulting in diverse photocatalysts. For instance, Song et al. constructed a Z scheme Ag_2CO_3/N-doped graphene photocatalyst. It demonstrated improved photocatalytic degradation of phenol (S. Song et al., 2017). Recently, Kalisamy et al. showed that the ZnO/S-doped g-C_3N_4 composite had enhanced charge separation and photocatalytic dye degradation ability (Kalisamy et al., 2020).

1.4 Synthesis protocol of doped photocatalysts

Nanosized photocatalysts are preferred because of their high surface area. The method used to fabricate the doped semiconductor could critically affect the extent of doping and nanostructure formation. The following techniques have been used to prepare doped photocatalysts.

1.4.1 Coprecipitation followed by calcination method

In this method (Arai et al., 2008; Aydın et al., 2019), precursor salts of the parent semiconductor and dopant are mixed in a solvent. The choice of the solvent should be such that it could appropriately dissolve both the precursor salts. Then, experimental parameters like temperature and pH are changed to precipitate the semiconductor phase. The as-prepared precipitate is subjected to a calcination process (high-temperature heating of solid precipitate) to get the crystalline phases of the semiconductor. During

this process, the dopant trapped in the precipitate can be included in the parent semiconductor lattice. For example, Mittal et al. (Mittal et al., 2014) prepared Cu-doped ZnO nanoparticles by this method. The homogeneous mixture of copper acetate, zinc acetate, and thioglycerol was treated with NaOH to increase its pH to 8. Then, the precipitate formed was dried and calcined at 300°C to obtain the final product.

1.4.2 Sol-gel method

In this technique, the precursor metal alkoxides are mixed to obtain a clear solution (Guglielmi & Carturan, 1988; Marami et al., 2018). Next, the solution is hydrolyzed to the corresponding metal hydroxide, which evolves into a lightweight gel. Sustained high-temperature heat treatments of the highly porous gels yield nanosized powder material. For example, Nithya et al. (Nithya et al., 2018) synthesized Nd-doped TiO_2 nanoparticles by this method. This material showed an antibacterial and photocatalytic property.

1.4.3 Reverse micelle method

This method proceeds through the formation of the micelles. At a particular concentration, the surfactant molecules aggregate in an arranged manner (hydrophilic and hydrophobic parts towards polar and nonpolar phases, respectively) and give micelles. In the reverse micelles, the orientation of the hydrophilic head and the hydrophobic tail are opposite to the normal micelles. The researchers exploited this method for the synthesis of doped semiconductors. Thus, this synthetic route has been used to prepare Eu^{3+} and Er^{3+}/Yb^{3+}-doped $GdVO_4$ nanoparticles (Gavrilović et al., 2014).

1.4.4 Solvothermal or hydrothermal method

Nowadays, solvothermal or hydrothermal methods are intensively used for doped photocatalyst preparation (Hong Li et al., 2017; Lupan et al., 2010). The reactant materials are dissolved in a solvent and then transferred to a sealed vessel (autoclave), with ~30% of its volume empty. The autoclave is then kept for high-temperature treatment. The temperature should be more than the boiling point of the taken solvent. Therefore, this high temperature generates an extreme condition of high internal pressure. The high temperature and autogenous high-pressure result in access to metastable doped crystal structures. The technique is called the hydrothermal method when water is the solvent. For instance, Viet et al. (Viet et al., 2018) synthesized Si-doped TiO_2 by such a protocol for the photocatalytic degradation of methylene blue (MB).

1.5 Synthesis of composites with doped photocatalysts

An extensive literature survey revealed only a few reports on synthesizing composites with doped materials. There are mainly two possible routes to fabricate this type of composite material with the help of the doped system. One way is to prepare the doped material first and then precipitate another component. For instance, following this route, the previously mentioned Ag_2CO_3/N doped grapheme composite was constructed. N-doped graphene sheets were first prepared, and then Ag_2CO_3 nanostructures were precipitated on them. Another technique involves preparing the doped system and the other component separately. Next, bind them by subjecting them to a hydrothermal or solvothermal protocol. Thus, Khalid et al. (Khalid et al., 2013) prepared Cu-doped TiO_2 and graphene separately, and then the mixture of these two systems was subjected to hydrothermal treatment at 120°C. In another publication, the solid from the homogeneous mixing of the g-C_3N_4 and Cd doped ZnO in an aqueous medium was

properly centrifuged and dried (Sher et al., 2021). After that, the mixture was subjected to high-temperature calcination at 580°C to get the g-C_3N_4/Cd-doped ZnO composite material.

1.6 Computational approaches to the doped photocatalysts

As discussed earlier, doping can significantly change the electronic structure of the parent semiconductor. The alterations of bandgap and band edge positions are due to the inclusion of the dopant in the lattice structure. The included dopant impurity can also destroy the lattice symmetry of the native semiconductor and alter the adsorption properties of the material (Bafekry et al., 2021; Y. Chen et al., 2018; Grishakov et al., 2020; Mushtaq et al., 2021; Sirikumara et al., 2016). Thus, the analysis of the effect of doping on the material's electronic structure is of keen interest to the researcher. Many experimental investigations are applied to determine the electronic structure of the doped semiconductor materials. For example, the high-resolution X-ray diffraction (HR-XRD) pattern of the doped semiconductor can indicate whether substitutional or interstitial doping has occurred. The different sizes of the dopant and occupying site can contract or expand the crystal lattice, which reflects in the positions of the XRD peak (Aydın et al., 2019; Moulahi, 2021; Pang & Abdullah, 2012; Tsuji et al., 2005). The optical bandgap of the material is measured by the UV visible diffuse reflectance spectroscopy (UV-DRS). It is noteworthy to mention that the optical bandgap is the energy difference between the VB and CB edges. The valence band XPS (VB-XPS) can examine the position of the VB edge directly from the spectrum. Thus, the combined study of VB-XPS and UV-DRS can give the band edges (VB and CB) position for a particular semiconductor (Ya Cui et al., 2019; Gansukh et al., 2020; Weikang Wang et al., 2019).

In this context, a computational investigation at the atomistic level enables us to validate the outcomes indicated by the experimental observations. Density functional theory (DFT) calculation using a plane-wave basis set is a perfect tool for determining the electronic structure of the doped systems. As discussed before, doping is mainly of two types, i.e., substitutional and interstitial. The DFT defect formation energy can tell us the feasibility of a particular type of doping (Finazzi et al., 2009; Tsin et al., 2015; Xinquan Wang et al., 2010). The minimum defect formation energy gives the more favorable doped (W. Yan & Liu, 2019; C. Zhou et al., 2020) crystal structure. For example, a DFT investigation showed that Si could substitute the Zn site in the ZnO lattice and lower formation energy (Körner & Elsässer, 2011). In addition, the DFT can describe the material's electronic density of states (DOS) (Sholl & Steckel, 2009). The lower and higher energy region corresponds to the VB and CB parts, separated by the Fermi level (zero energy level) (see Figure 1.4). The flat portion (with no energy states) in the neighborhood of the Fermi region gives the material's bandgap. The DFT-generated band structure can also give the bandgap. Note that the DOS and band structure are collected from the optimized geometrical structure of the material.

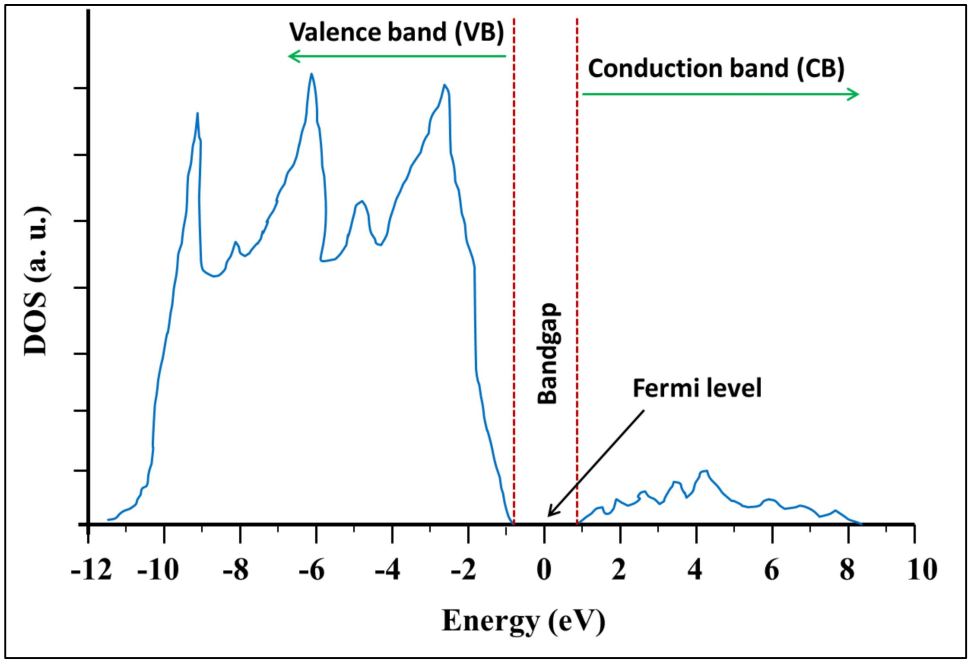

Figure 1.4 A typical DOS plot of a semiconductor material.

1.7 Research gap

Ag_2O is a semiconductor photocatalyst with a bandgap range of 1.2-1.5 eV. This narrow bandgap restricts its photocatalytic ability. The same small bandgap is also an advantage when one considers that it can absorb almost all of the UV-visible range of the solar spectrum. But, pure Ag_2O also faces photo-stability and recombination issues during photocatalysis (H. Xu et al., 2018). A frequent observation is the conversion of Ag^+ into Ag during the use of Ag_2O as a photocatalyst under visible light. When Ag_2O is exposed to visible light, the photo-generated electrons transfer to the neighboring Ag^+ in the lattice, rather than to O_2 in the aqueous environment. It happens because the $E^0_{O_2/HO_2}$= -0.046 V (vs SHE scale) is more negative than $E^0_{Ag^+/Ag}$= 0.799 V reduction potential. Hence, the formation of metallic Ag on the Ag_2O surface is natural. Hereafter, the (Ag_2O) photo-excited electrons are transferred to adjacent Ag clusters. Here, it is vital to note the excellent oxygen affinity of Ag clusters. Thus, the oxygen molecules

adsorbed on the Ag structures are reduced by the transferred photo-excited electrons. Two-electron oxygen reduction can result in H_2O_2 formation. The electrons on Ag structures can also get excited plasmonically and result in superoxide radical formation. On the other hand, the reactive holes oxidize the organic contaminants rather than lattice O^{2-} and enhance the stability of the Ag-O-Ag crystal structure. In this way, the metallic Ag clusters function as co-catalysts and resolve the photo-stability issues of Ag_2O. Essentially, proper charge separation in the material can resolve these problems. As discussed earlier, either doping or heterostructure formation with the pure single-phase semiconductor can create an efficient charge separation in the material. There are many reports on the construction of heterostructures with Ag_2O as one of the components. For instance, Ag/Ag_2O/reduced TiO_2, Ag_2O/WO_3, Curcumin/Ag/Ag_2O, Ag_2O/Ag_3PO_4, Ag_2O/Bi_2O_3, etc. have been synthesized and found to possess efficient photocatalytic (Yuqi Cui et al., 2017b; Jo et al., 2020; S. Kumar et al., 2018a; P.-Q. Wang et al., 2013; L. Zhu et al., 2012) activities towards specific organic molecules. To our knowledge, only one report is available in the literature on doped Ag_2O. This report is on preparing Sr-doped Ag_2O nanostructures for photocatalytic degradation of organic pollutants (Kiani et al., 2019).

There are a few computational investigations (plane-wave DFT calculations) reported on the pure Ag_2O. For example, Pei et al. calculated a 0.08 eV (approximately zero) bandgap for Ag_2O using GGA-PBE functional, much smaller than the experimentally investigated bandgap (1.2 – 1.5 eV). Although DFT calculations using this functional can give general information about the band structure, it underestimates the actual bandgap of the material (F. Pei et al., 2009). But, using a suitable hybrid functional (HSE06) can result in an appropriate bandgap, which is similar to the experimental one (Allen et al., 2011). Note that such hybrid functional is

computationally very costly and requires high computational resources. In another recent investigation, Ribeiro et al. analyzed the details electronic structure of Ag_2O photocatalyst by a systematic DFT study (Ribeiro et al., 2020). In this study, the authors found the energetically stable Ag_2O surface, where photocatalysis occurs. DFT calculations have been performed on Ag_2O crystal structure with defects. For example, Yin et al. introduced point defects in cuprite Ag_2O and investigated structural and electronic properties changes due to the incorporated defects. Different Ag and O-rich conditions were induced in the system by creating Ag or oxygen vacancies in the supercell. It was found that the Ag-rich condition required a higher formation energy value than the O-rich condition (Yin et al., 2016). It must be mentioned that before this thesis, no plane-wave DFT calculation investigations have been reported on doped Ag_2O nanomaterials in the literature.

1.8 Objectives of the thesis

The extensive literature survey in the previous section shows many publications on composites with pure Ag_2O to overcome typical photocatalysis efficiency issues. Introducing a cationic or anionic dopant in pure Ag_2O is hardly reported in the existing literature. Therefore, the limited knowledge of the effect of dopants in Ag_2O photocatalyst on its electronic structure and photocatalytic activity inspired the following objectives of the thesis.

(i) Preparation and characterization of Zn-doped Ag_2O nanoparticles to understand how the dopant affects the nanoparticle's lattice structure. Investigation of the effect of doping on bandgap and photocatalytic properties towards an organic pollutant. Parallel DFT investigations to find

the stable doped crystal structure and impact of Zn-doping on band structure and DOS of Ag_2O.

(ii) The second objective was to incorporate Ni dopant in the Ag_2O nanoparticles and investigate its influence on the nanoparticle's bandgap and photocatalytic properties. The analogous computational studies also validate the experimental findings.

(iii) The next objective was to investigate the effect of the anion (sulfur) S-doping on the Ag_2O lattice structure. Computational studies were also performed to uphold the experimental results.

(iv) The fourth objective of the thesis was to construct a composite with a doped Ag_2O system. In this regard, the first part is to prepare Cd-doped Ag_2O and $BiVO_4$ nanoparticles separately. Next, use these components to prepare and characterize Cd-doped $Ag_2O/BiVO_4$ composites and investigate their photocatalytic properties. Simultaneously, DFT investigations have been carried out to find the stable Cd-doped crystal structure. The DFT investigation of adsorption of H_2O and O_2 molecules on Cd doped Ag_2O and $BiVO_4$ surfaces have also been used to elucidate the photocatalytic mechanism.